JBC RESEARCH ARTICLE

A mechanochemical model of the forward/backward movement of motor protein kinesin-1

Received for publication, January 28, 2022, and in revised form, April 11, 2022 Published, Papers in Press, April 18, 2022,
https://doi.org/10.1016/j.jbc.2022.101948

Beibei Shen and Yunxin Zhang*

From the Shanghai Key Laboratory for Contemporary Applied Mathematics, School of Mathematical Sciences, Fudan University, Shanghai, China

Edited by Enrique De La Cruz

Kinesin-1 is an ATP-driven, two-headed motor protein that transports intracellular cargoes (loads) along microtubules. The movement of kinesin-1 has generally been modeled according to its correlation with ATP cleavage (forward movement), synthesis (backward movement), or unproductive cleavage (futile consumption). Based on recent experimental observations, we formulate a mechanochemical model for this movement in which the forward/backward/futile cycle can be realized through multiple biochemical pathways. Our results show that the backward motion of kinesin-1 occurs mainly through backward sliding along the microtubule and is usually also coupled with ATP hydrolysis. We also found that with a low external load, about 80% of ATP is wasted (futile consumption) by kinesin-1. Furthermore, at high ATP concentrations or under high external loads, both heads of kinesin-1 are always in the ATP- or ADP · Pi-binding state and tightly bound to the microtubule, while at low ATP concentrations and low loads, kinesin-1 is mainly in the one-head-bound state. Unless the external load is near the stall force, the motion of kinesin-1 is almost deterministic.

Kinesin-1 plays a central role in the intracellular transport of various vesicles and organelles (1–4). Each kinesin-1 dimer consists of two motor domains (heads), which are connected to a coiled-coil stalk through a ∼ 14-amino-acid-long sequence known as the neck linker (NL) (5–9). Kinesin proceeds unidirectionally toward the plus ends of a microtubule (MT) by an asymmetric hand-over-hand fashion, hydrolyzing an ATP molecule for each 8-nm step (10–16). Motion of kinesin-1 is significantly processive (17, 18), taking about 100 steps before detaching from the MT (1, 19, 20). At low loads, kinesin-1 always steps forward to the plus ends of the MT, while at high loads, it can also result in backward steps (21–23).

In previous studies, kinds of theoretical models have been presented to understand the mechanism of kinesin-1 motion (refer to the studies by Parrondo and Cisneros (24), Kolomeisky and Fisher (25), Chowdhury (26), and Mugnai and Hyeon (27) for details). Generally, the motion of kinesin-1 can be regarded as a Markov process with multiple biophysical and biochemical states, and in a steady state, meaningful quantities can be obtained by using the Fokker–Planck equation, master equation, Langevin dynamics, or any other complicated hybrid models (28, 29). Among most of these models, a backward step of kinesin-1 is usually thought to occur by directional reversal of a forward step and therefore happens with ATP synthesis.

Generally, both forward and backward steps of kinesin-1 may be accomplished through different biochemical pathways, and backward motion of kinesin-1 may be resulted simply from pure biophysical slips along the MT (30). According to a mechanochemical model (see Fig. 1), this study shows that there are two biochemical pathways for forward step. At low ATP concentration and low external load, kinesin-1 will spend more time waiting for ATP, and its MT-bound head might be in the nucleotide-free state. However, at high ATP concentration or high external load, all MT-bound heads are usually in ATP or ADP · Pi-binding state, and ATP binding to the front head of kinesin-1 is earlier than the release of Pi and the detachment of the trailing head from the MT. There are altogether six possible pathways for backward motion, unless at some extreme conditions the backward motion of kinesin-1 is through backward slips along the MT when it is in a semidetach state and usually coupled with ATP hydrolysis. Directional reversal of forwarding pathways is only non-negligible when the ATP molecule is scarce, while the external load is very high. One surprising finding is that about 80% of ATP is wasted by kinesin-1, and this proportion of waste is almost independent of ATP concentration.

Results

Biophysics of kinesin-1 motion along the MT

Using parameter values listed in Table 1, our model can reproduce the related experimental results well (see Fig. 2). For detailed methods of theoretical predictions, see the supplemental information. In the following, we will always use parameter values listed in Table 1 to discuss the mechanochemical properties of kinesin-1.

From Table 1, $\delta_{23}+\delta_{32} \approx 0.47$, which implies that there may be two substeps within each 8-nm step of kinesin-1, with size 3.76 nm and 4.23 nm, respectively, as previously observed in the studies by Coppin et al (31) and Nishiyama et al (32). According to Figure 1*A*, these two substeps are caused by binding of the nucleotide-free head to the front site of the MT and detachment of the ADP-bound rear head from the MT,

* For correspondence: Yunxin Zhang, xyz@fudan.edu.cn.

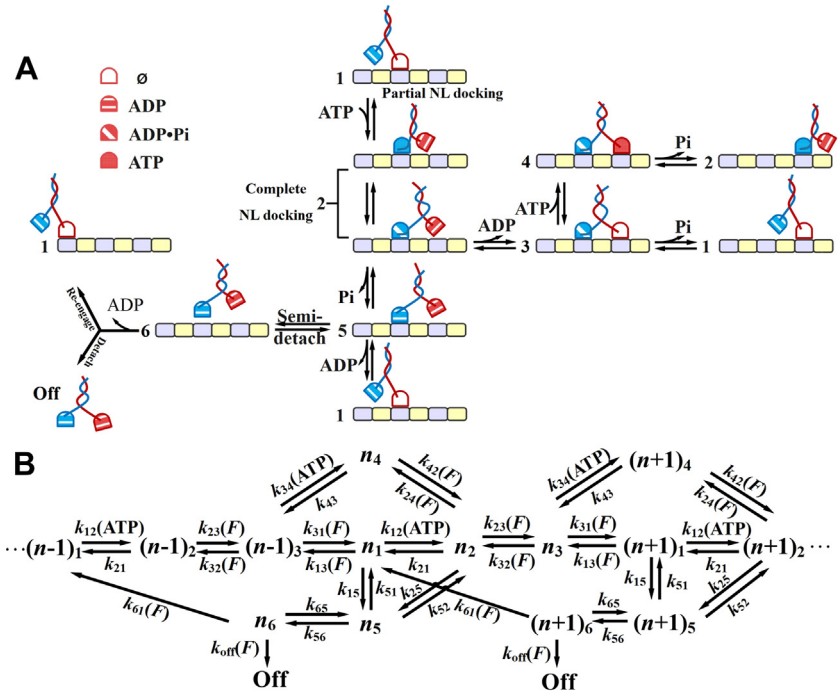

Figure 1. The mechanochemical model of kinesin-1. *A*, the depiction of detailed configurations of the two heads of kinesin-1. There are six possible configurations at each binding site of the MT. *B*, mechanochemical model used in this study to describe the periodic motion of kinesin-1, where n_j denotes the state that kinesin-1 is at position n and in configuration j, with $j = 1, 2, \cdots, 6$. MT, microtubule.

respectively. But, for high ATP concentration, rates k_{12}, k_{34}, and k_{23} are very large and the substep coupled with transition $2 \rightleftharpoons 3$ is difficult to be observed in experiments.

The load distribution factor $\delta_{31} = 0$ means the energy barrier between state 3 and 1 is very close to state 3. Transition rate k_{31} is independent of external load F, while k_{13} increases rapidly with F. The process $4 \rightleftharpoons 2$ is similar since $\delta_{42} = 0.006$ is also very small.

Figure 3, *A* and *D* show that, at low load F and low ATP concentration [ATP], kinesin-1 mainly stays in biochemical state 1, *i.e.*, with only one nucleotide-free head bound to the MT while the other ADP-bound head detached. At high ATP concentration, kinesin-1 stays mainly in state 4, with both heads in ATP or ADP · Pi-bound state and bound to the MT tightly. Meanwhile, if the load F is not high, the probability that kinesin-1 in the two ADP-bound state 5 is also relatively high (about 1/5) (see Fig. 3, *A*, *B* and *E*). At low [ATP] while high load F, kinesin-1 stays mainly in state 3 with both two heads bound to the MT but one in nucleotide-free state (see Fig. 3, *C* and *D*). Provided the load F is high, kinesin-1 stays mainly in two head-bound states and stays mainly in state 4 when [ATP] is high and in state 3 otherwise (see Fig. 3*C*).

Generally, probability ρ_1 decreases while $\rho_2, \rho_4, \rho_5, \rho_6$ increases with ATP concentration. At high load F, ρ_3 decreases with [ATP] monotonically; otherwise, ρ_3 may increase first and then decrease with [ATP]. At low ATP concentration, kinesin-1 mainly stays in the ATP waiting state 1 or 3. But with the increase of load F, kinesin-1 switches from the one head-bound state 1 to the two-head-bound state 3 (see Fig. 3, *A*–*D*). When ATP concentration is high, all probabilities ρ_i change only slightly with the load F (see Fig. 3*E*).

Figure 3*F* shows the stall force F_s, under which the mean velocity of kinesin-1 vanishes, increases slightly with ATP concentration and eventually approaches to a constant between 7 and 8 pN, which agrees well with experimental measurements (33–35).

Figure 4, *A* and *B* show the mean run time $\langle t \rangle$ of kinesin-1 decreases with ATP concentration monotonically, while it first decreases slightly and then increases rapidly with load F. These results seem surprising. One possible explanation is that, in general, kinesin-1 does not detach from the MT unless it has transported its cargo to the corresponding destination (18, 36). So, with low ATP concentration, kinesin-1 will stay on the MT for more time, since the period of single biochemical cycle becomes long due to the lack of ATP molecule. Actually, Figures 4*B* and 2*B* show both mean run time $\langle t \rangle$ and mean run length $\langle l \rangle$ tend to limit constants at high ATP concentration.

Table 1
Model parameter values obtained by fitting to experimental data of kinesin-1 purified from wildtype *Drosophila* measured in the studies by Schnitzer et al (44) Visscher et al (33), see Figures 1 and 2

Parameter	Value	Parameter	Value
k_{12}^0, k_{34}^0	9.827 μM^{-1} s^{-1}	k_{21}, k_{43}	5074.875 s^{-1}
k_{23}^0	1627.099 s^{-1}	δ_{23}	0.055
k_{32}^0	0.006 s^{-1}	δ_{32}	0.416
k_{31}^0, k_{42}^0	137.582 s^{-1}	δ_{31}	0
δ_{42}	0.006	k_{31}^0, k_{24}^0	1.666 s^{-1}
δ_{13}	0.529	δ_{24}	0.523
k_{25}^0	5146.371 s^{-1}	k_{52}^0	77.252 s^{-1}
k_{15}^0	4.344 s^{-1}	k_{51}^0	1455.909 s^{-1}
k_{56}^0	345.215 s^{-1}	k_{65}^0	2923.252 s^{-1}
k_{61}^0	0.001 s^{-1}	k_{off}^0	5.286 s^{-1}
d_{off}	0.803 nm		

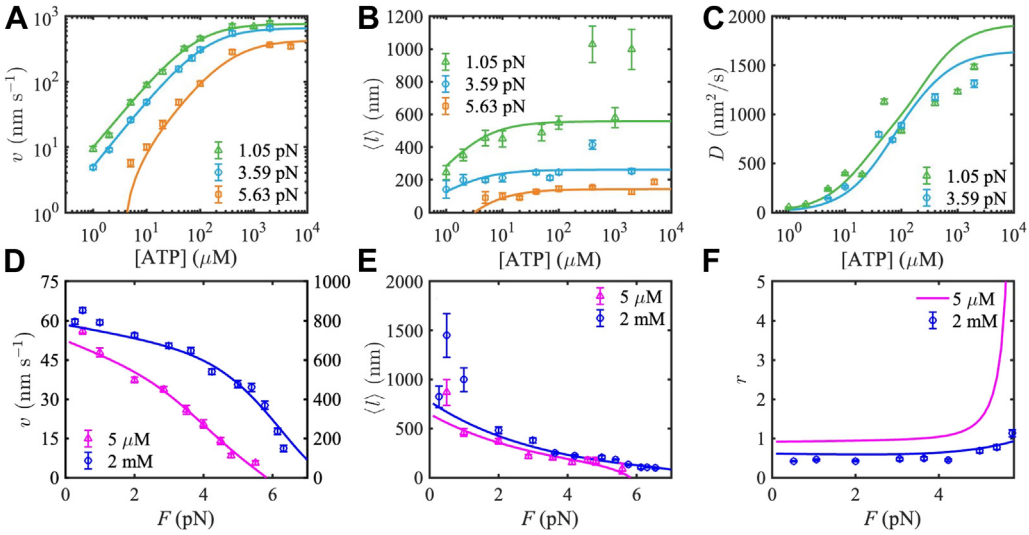

Figure 2. Theoretical predictions (*solid lines*) and experimental data (markers) of various biophysical properties of kinesin-1 purified from wildtype *Drosophila*. *A–E*, the data in (*A*, *B*, *D*, and *E*) are from the study by Schnitzer et al (44), and in (*C* and *F*) are from the study by Visscher et al (33). In (*D*), the *left* axis is for 5 μM ATP, while the *right* axis is for 2 mM ATP. v is the mean velocity of kinesin-1 along the MT, $\langle l \rangle$ is the mean run length of kinesin-1 before its detachment from MT, r is the randomness, and D is the diffusion constant which is estimated from $r = 2D/vd$ with $d = 8$ nm the step size of kinesin-1. For methods of theoretical predictions, see the supplemental information. MT, microtubule.

Possibly, in cells, such run time/length is enough to transport any cargoes to their corresponding destinations. At low ATP concentration and high external load, $\langle t \rangle$ increases with F, which implies kinesin-1 will try to run more time along the MT to complete its task when its motion is slowed down by resistance (see Fig. 4, *A* and *B*).

Generally, both mean value $\langle l \rangle$ and variance $\mathrm{Var}(l)$ decrease with load F. If F is not too large, both $\langle l \rangle$ and $\mathrm{Var}(l)$ increase with [ATP] (see Figs. 2, *B* and *E*, 4*C*, and S1*D*). The variance of run time $\mathrm{Var}(t)$ decreases with ATP concentration, while it decreases first and then increases with the load F (see Figs. 4*D* and S1*A*). Further calculations show both coefficient of variation $\mathrm{CV}_l := \langle l \rangle / \sqrt{\mathrm{Var}(l)}$ and $\mathrm{CV}_t := \langle t \rangle / \sqrt{\mathrm{Var}(t)}$ almost equal to 1 (see Fig. S1, *B*, *C*, *E* and *F*). So both the run time of kinesin-1 along the MT and its run length are approximately exponentially distributed.

The mean run time $\langle t \rangle$ is actually the time spent by kinesin-1 in average to detach from the MT. So, $\langle t \rangle$ is related to probability flux of detachment $\mathrm{flux}_{\mathrm{off}} := k_{\mathrm{off}} \rho_6$. Intuitively, $\mathrm{flux}_{\mathrm{off}}$ should change with F and [ATP] in a similar manner as $1/\langle t \rangle$. In contrast to Figure 4, *A*, *B*, *E* and *F* show detachment flux $\mathrm{flux}_{\mathrm{off}}$ increases monotonically with [ATP], while it increases first and then decreases with load F.

Pathways of forward/backward/futile biochemical cycle of kinesin-1

Given the model depicted in Figure 1, there is no evident information about the coupling between the biochemical cycle

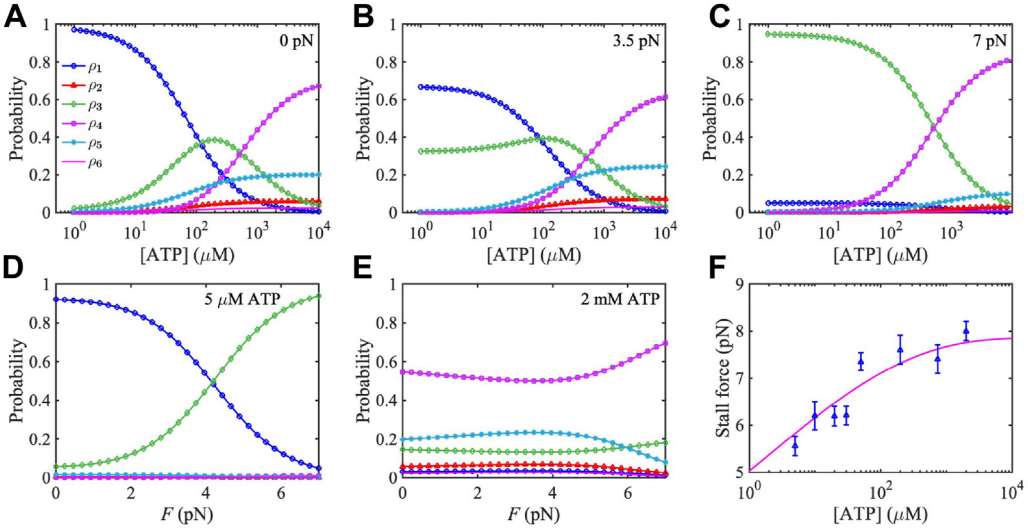

Figure 3. Probability ρ_i of kinesin-1 in the six biochemical states. *A–C*, probability ρ_i of kinesin-1 in the six biochemical states as depicted in Figure 1, *versus* ATP concentration [ATP] at different load. *D–E*, probability ρ_i of kinesin-1 *versus* load F at different ATP concentrations. *F*, stall force of kinesin-1 as a function of [ATP], where the solid line shows the theoretical predictions using parameters listed in Table 1, and triangles denote experimental data measured in the study by Visscher et al (33).

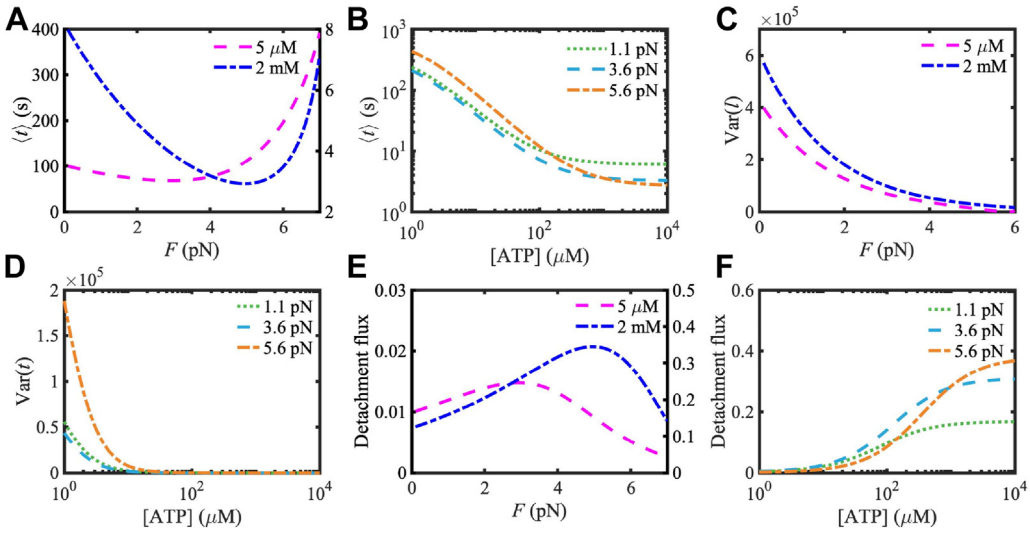

Figure 4. Mean and variance of run time *t* and run length *l* of kinesin-1 along MT. *A* and *B*, mean run time $\langle t \rangle$ with the change of load *F* and [ATP]. *C*, variance of run length $\mathrm{Var}(l)$ with the change of *F*. *D*, variance of run time $\mathrm{Var}(t)$ with the change of [ATP]. *E–F*, probability flux of kinesin-1 detachment from the MT, $\mathrm{flux}_{\mathrm{off}} := k_{\mathrm{off}}\rho_6$, with the change of load *F* and [ATP]. In (*A* and *E*), the *left* axis is for [ATP] = 5 μM and *right* axis is for [ATP] = 2 mM. For methods of theoretical predictions of $\langle t \rangle$, $\mathrm{Var}(l)$, and $\mathrm{Var}(t)$, see the supplemental information. MT, microtubule.

of ATP hydrolysis and mechanical step of kinesin-1. As pointed out before, there are generally three categories of the biochemical cycle, *forward/backward/futile* cycle. Mean velocity v is actually the sum of probability fluxes of different biochemical cycles, weighted by mechanical step size. It is generally difficult to sort out these three categories of biochemical cycle and then calculate their corresponding fluxes since net flux between any two adjacent biochemical states i and j, $\mathrm{flux}_{ij} := k_{ij}\rho_i - k_{ji}\rho_j$, usually changes with external load F and ATP concentration [ATP]. Fortunately, thorough numerical calculations show that, with parameter values listed in Table 1 and biophysically meaningful load F and [ATP], there are only five different cases for probability flux and in each case, the direction of net flux between any two adjacent states does not change (see Figs. S2–S4). For each case, *forward/backward/futile* cycle can be phenomenologically sorted out by analyzing all possible biochemical pathways. The results are summarized in Table 2.

At low load F, the flux of *backward* cycle flux_- is negligible, indicating the impossibility of backward motion (18, 36) (see Figs. 5, *A*, *B*, *D* and *E*, S5). Both *forward* flux flux_+ and *futile* flux flux_0 increase with [ATP]. At low load F, proportions of flux_+ and flux_0 are almost independent of [ATP], which implies that the utilization ratio of ATP is independent of [ATP] (see Fig. 5, *D* and *E*). At super stall load, kinesin-1 motion is dominated by *backward* cycle when [ATP] is small, while it is dominated by *futile* cycle when [ATP] is large. Particularly, for $F = 8$ pN, the proportion of *backward* flux flux_- is almost 1 when [ATP] <22.23 μM, indicating that kinesin-1 moves backward almost deterministically. For large enough [ATP], the lower limit value of the proportion of flux_- is almost the same as the upper limit value of the proportion of flux_+, so the motion of kinesin-1 is completed stalled (see Fig. 5, *C* and *F*). With increasing [ATP], the proportion of flux_0 rises rapidly, until 263.47 μM, at which the sign of flux_{23} changes from negative to positive, switching from **Case 3** to **Case 2**, producing the flux of *forward* cycle $\mathrm{flux}_+ > 0$ (see Figs. S3*C*, 5, *C* and *F*). On the whole, at high load and low ATP concentration, kinesin-1 can only move backward. As [ATP] increases, the futile flux begins to rise rapidly, and then forward flux is generated. For large enough [ATP], *backward* flux is balanced by *forward* flux, and the motion of kinesin-1 is stalled completely.

Further calculations show that both *forward* flux flux_+ and its proportion decrease, while the proportion of flux_- increases, with load F, which implies the utilization ratio of ATP decreases with load F (see Fig. S5). At [ATP] = 5 μM and [ATP] = 2 mM, the intersection points of flux_+ and flux_- are found at $F = 5.85$ pN and $F = 7.76$ pN, respectively, which are exactly the stall forces F_s of kinesin-1 at [ATP] = 5 μM and [ATP] = 2 mM (see Fig. 3*F*). One surprising result is that, except the extreme cases with high load F and very low [ATP], the biochemical process of kinesin-1 is mainly dominated by *futile* cycle, and utilization ratio of ATP is only about 20% (see Fig. 5). At low load F, the *backward* flux is almost zero. While for load F larger than stall force, the *forward* flux decreases rapidly to zero. This indicates that, unless at external load which is near the stall force, the motion of kinesin-1 is almost deterministic. At low load, kinesin-1 hardly steps backward (18). This is different with the conclusion drawn from Brownian ratchet models (37, 38).

Forward cycle consists of two possible pathways, $\overrightarrow{1231}$ and $\overrightarrow{2342}$, both of which include hydrolysis of one ATP and a forward mechanical step of 8 nm (see Table 2). *Futile* cycle consists of two possible pathways, $\overrightarrow{1251}$ and $\overrightarrow{134251}$, both of which include hydrolysis of one ATP but without a mechanical step. *Backward* cycle consists of six possible pathways, which are $\overrightarrow{12561}$, $\overrightarrow{1342561}$, $\overrightarrow{13251}$, $\overrightarrow{132561}$, $\overrightarrow{2432}$, and $\overrightarrow{1321}$. These six pathways can be further classified into three categories, **(i)** $\overrightarrow{12561}$ and $\overrightarrow{1342561}$, which are mainly induced by backward sliding 6 → 1 through the semidetach state, **(ii)** $\overrightarrow{13251}$, $\overrightarrow{2432}$,

Table 2
Pathway details of *forward/backward/futile* biochemical cycle of kinesin-1

Conditions	Cycles	Pathway	ATP	Steps	Total flux
+ + ++ (Case 1)	Forward	$\overrightarrow{1231}$	1	1	flux23
		$\overrightarrow{2342}$	1	1	
	Backward	$\overrightarrow{12561}$	1	−1	flux61
	Futile	$\overrightarrow{1251}$	1	0	flux51
− + ++ (Case 2)	Forward	$\overrightarrow{2342}$	1	1	flux23
	Backward	$\overrightarrow{12561}$	1	−1	flux61
		$\overrightarrow{1342561}$	1	−1	
	Futile	$\overrightarrow{1251}$	1	0	flux51
		$\overrightarrow{134251}$	1	0	
− − ++ (Case 3)	Forward	—	—	—	0
	Backward	$\overrightarrow{12561}$	1	−1	$\text{flux61} + \text{flux51}\frac{flux32}{flux25}$
		$\overrightarrow{1342561}$	1	−1	
		$\overrightarrow{13251}$	0	−1	
		$\overrightarrow{132561}$	0	−2	
	Futile	$\overrightarrow{1251}$	1	0	$\text{flux51}\frac{flux12+flux42}{\text{flux25}}$
		$\overrightarrow{1251}$	1	0	
− − − + (Case 4)	Forward	—	—	—	0
	Backward	$\overrightarrow{12561}$	1	−1	$\text{flux61} + \text{flux24} + \text{flux51}\frac{flux13}{\text{flux25}}$
		$\overrightarrow{132561}$	0	−2	
		$\overrightarrow{13251}$	0	−1	
		$\overrightarrow{2432}$	−1	−1	
	Futile	$\overrightarrow{1251}$	1	0	$\text{flux51}\frac{flux12}{\text{flux25}}$
− − − − (Case 5)	Forward	—	—	—	0
	Backward	$\overrightarrow{1321}$	−1	−1	$\text{flux32} + \text{flux61}$
		$\overrightarrow{132561}$	0	−2	
		$\overrightarrow{2432}$	−1	−1	
	Futile	$\overrightarrow{13251}$	0	−1	
			—	—	0

Column 'Conditions' lists the signs of flux_{31}, flux_{23}, flux_{34}, and flux_{12}, respectively. Column 'ATP' lists the number of ATP molecule consumed in the corresponding pathway, where '− 1' means one ATP is synthesized. Column 'Steps' gives the number of mechanical step coupled with the pathway, with one step 8 nm. Column 'Total flux' lists the total flux of the *forward/backward/futile* cycle. $\overrightarrow{ij\cdots ki}$ denotes the biochemical pathway $i \to j \to \cdots \to k \to i$. It is evident from Figure 1 that $\text{flux}_{42} = \text{flux}_{34}$. Flux flux_{25}, $\text{flux}_{56} = \text{flux}_{61}$, and flux_{51} are always nonnegative for $0 \le F \le 9$ pN and 1 μM ≤ [ATP] ≤ 10,000 μM, see Fig. S2.

and $\overrightarrow{1321}$, which can be roughly regarded as the reversal of corresponding *forward* pathways, and **(iii)** $\overrightarrow{132561}$, which includes both the reversal of a forward pathway and the backward sliding 6 → 1, and therefore coupled with a backward motion of total 16 nm. Pathway $\overrightarrow{2432}$ and $\overrightarrow{1321}$ include the synthesis of ATP, while $\overrightarrow{12561}$ includes the hydrolysis of ATP. Note that pathway $\overrightarrow{ij\cdots ki}$ can be denoted equivalently as $\overrightarrow{j\cdots kij}$, $\overrightarrow{kij\cdots k}$, etc. For convenience, we denote the probability flux through pathway $\overrightarrow{ij\cdots ki}$ by $f_{\overrightarrow{ij\cdots ki}}$.

With small [ATP] and load $F \ll F_s$, the *forward* cycle is mainly realized through pathway $\overrightarrow{1231}$ (see Figs. S6, *A* and *D*, S8, *A* and *D*, S9, *A* and *D*). Otherwise, the *forward* cycle is mainly realized through pathway $\overrightarrow{2342}$ (Figs. S6–S10, *A* and *D*). During pathway $\overrightarrow{2342}$, binding of ATP to the front head of

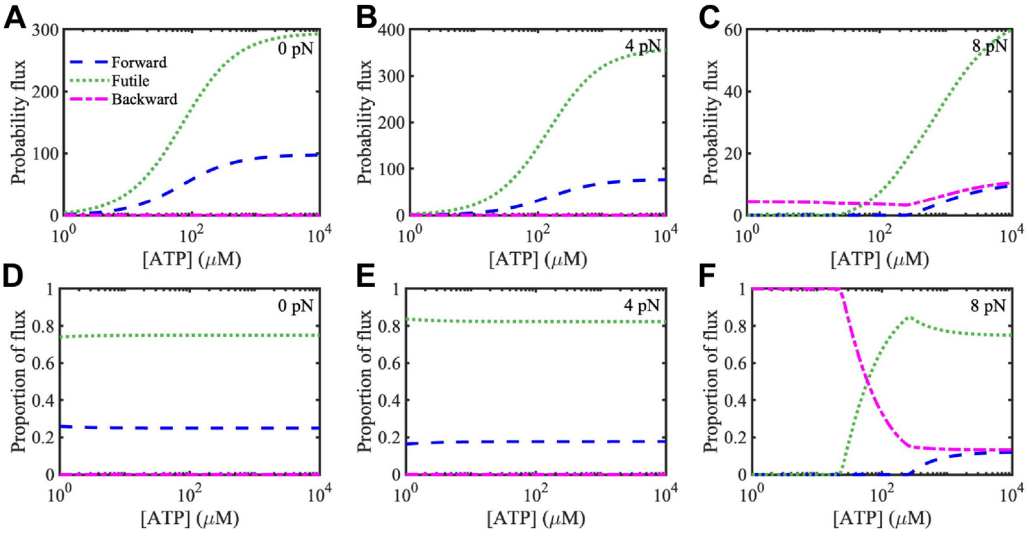

Figure 5. Probability flux of *forward/backward/futile* cycle of kinesin-1, as well as their proportions, *versus* [ATP], with load $F = 0$ pN, 4 pN and 8 pN, respectively.

kinesin-1 is earlier than the release of phosphate Pi from the rear head, while during pathway $\overrightarrow{1231}$, ATP binds to the front head only after the detachment of rear head from the MT. So, our results imply that at low external load and low ATP concentration, the MT-bound head might be in the nucleotide-free state, while at high ATP concentration or high load, the head bound to the MT is always in ATP or ADP · Pi-binding state. This is consistent with results shown in Figure 3.

Except some extreme cases, *futile* cycle is mainly realized through pathway $\overrightarrow{1251}$. Moreover, for small load F or small [ATP], the probability that the *futile* cycle is realized through $\overrightarrow{134251}$ is almost negligible (see Figs. S6–S10, *B* and *E*).

If load F is small, *backward* cycle is mainly realized through pathway $\overrightarrow{12561}$ and other pathways are all negligible (see Figs. S6–S9, *C* and *F*). If both F and [ATP] are large, the *backward* cycle is mainly realized through pathway $\overrightarrow{12561}$ and pathway $\overrightarrow{1342561}$ and also with $\overrightarrow{12561}$ the most prominent one (see Figs. S7, *C* and *F*, S10, *C* and *F*). If F is large but [ATP] is small, pathways $\overrightarrow{13251}$, $\overrightarrow{2432}$, $\overrightarrow{1321}$, and $\overrightarrow{132561}$ are all important, while both pathway $\overrightarrow{12561}$ and pathway $\overrightarrow{1342561}$ are negligible (see Figs. S6, *C* and *F*, S10, *E* and *F*). For large F and small [ATP], prominent pathways of *backward* cycle are roughly related to the reversal of corresponding pathways of *forward* cycle and consequently might lead to the synthesis of ATP (see Table 2). However, this is difficult to observe experimentally since kinesin-1 may have already detached from the MT before achieving such harsh conditions.

During pathways $\overrightarrow{12561}$ and $\overrightarrow{1342561}$, backward motion of kinesin-1 is induced only by the backward sliding of 8 nm through transition 6 → 1. But during pathway $\overrightarrow{132561}$, the backward motion is accomplished by both one backward sliding of 8 nm and one backward step of 8 nm. Figure 6 shows that the probability flux through pathway $\overrightarrow{132561}$ is very rare and the backward step of 16 nm is observable only under the very harsh condition that external load F is high but ATP is scarce. If ATP concentration reach saturating, both probability flux of 8-nm backstep and 16-nm backslip decrease to zero, with only backslip 8 nm existing (see Fig. 6, *B* and *C*).

Discussion

A mechanochemical model of kinesin-1 is constructed, in which the motor can step forward/backward through multiple biochemical pathways. Biophysical meaningful quantities of kinesin-1, including its mean velocity, diffusion constant, and mean run time/length, are obtained theoretically.

Our study shows that mean run time of kinesin-1 along the MT decreases with ATP concentration monotonically and finally tends to an external load-dependent limit value but decreases first and then increases rapidly with external load, which are different with properties of the mean run length observed in experiments. However, both distributions of run time and run length are approximately exponential.

Forward motion of kinesin-1 can be realized through two possible biochemical pathways. At high ATP concentration or under high external load, the kinesin head bound to the MT will always be in ATP or ADP Pi-binding state. But at low ATP concentration and low load, new ATP molecule will not bind to the nucleotide-free head before the release of phosphate Pi and the detachment of the trailing head from the MT. Kinesin-1 may stay at the one-head-bound state for a long time to wait for ATP arrival.

Backward motion of kinesin-1 is mainly caused by backward sliding along the MT through a semidetach state and hardly through directional reversal of forward pathways as usually believed in previous studies. Large backward step and directional reversal of forward pathways can only happen in very harsh environments with scarce ATP molecules but under high external load. Usually, kinesin-1 has already been pulled down from the MT before achieving such conditions.

One surprising finding is that the utilization ratio of ATP is only about 20%, and about 80% of ATP is consumed in the futile cycle, which consists of two possible biochemical pathways.

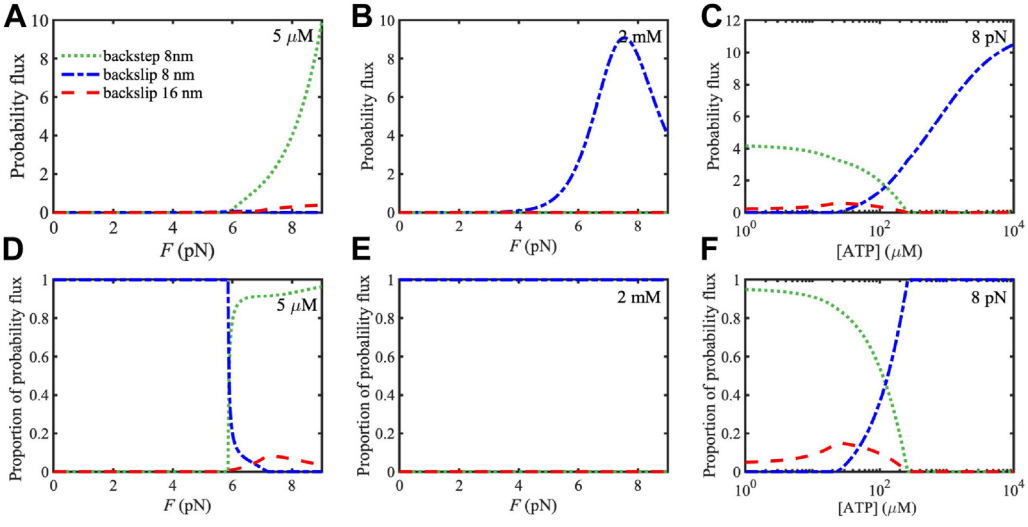

Figure 6. Probability flux of 8-nm backstep, 8-nm backslip, and 16-nm backslip, as well as their corresponding proportions at various [ATP] and load *F*. (*A–C*) show the probability flux at [ATP] = 5 μM, [ATP] = 2 mM, and F = 8 pN, respectively, and (*D–F*) show their corresponding proportions. The flux of 8-nm backstep is obtained by $f_{\overrightarrow{13251}}+f_{\overrightarrow{2432}}+f_{\overrightarrow{1321}}$, the flux of 8-nm backslip is obtained by $f_{\overrightarrow{12561}}+f_{\overrightarrow{1342561}}$, and the flux of 16-nm backslip is $f_{\overrightarrow{132561}}$.

Unless ATP concentration is extremely low but external load is high, ATP is required in almost all backward steps of kinesin-1, though these backward steps are mostly accomplished through the sliding process in its semidetach state.

Experimental procedures

Based on experimental observations in the study by Toleikis et al (30), this study uses the mechanochemical model as depicted in Figure 1. The biochemical cycle of kinesin-1 is assumed to begin with the one-head-bound, ATP-waiting state, with the nucleotide-free front head tightly bound to the MT while the ADP-bound rear head unbound (39). ATP binding induces NL docking, and ATP hydrolysis completes NL docking (5, 7, 8) (see Fig. 1*A* 1 → 2). In either ATP or ADP Pi-bound states, the head binds tightly to the MT, so these two states are assumed to be the same and denoted as state 2 in Figure 1. Due to NL docking, the unbound head of kinesin-1 swings forward and becomes the front head. ADP release facilitates front head binding to the MT, leading kinesin-1 changes from state 2 to state 3, generating a two-head-bound state. At low ATP concentration, the release of phosphate ion Pi from the rear head usually occurs before an ATP molecule reaches the newly bound front head. Then dissociation of the ADP-bound rear head from the MT leads kinesin-1 to return to the biochemical state 1 again. However, if ATP concentration reaches saturation, after ADP releases from the front head, another ATP molecule will bind to the nucleotide-free head immediately, leading kinesin-1 to enter the biochemical state 4. Next, the release of Pi from the rear head leads kinesin-1 to return to state 2. In either case, 1 → 2→ 3→ 1 or 2→ 3→ 4→ 2, one biochemical cycle of kinesin-1 is completed once the ADP-bound rear head dissociates from the MT. Meanwhile, kinesin-1 makes an 8-nm forward step along the MT and is ready to start a new mechanochemical cycle again (12, 13, 15).

Recent experiments discovered that backward step originates from a different and later state in the biochemical cycle than the one that generates forward steps, and backward step and detachment might emanate from the same state (30). So, our model assumes that forward step can only occur before Pi release from the ADP · Pi-bound head (see state 2 in Fig. 1), whereas backward step/slipping and detachment can only occur after Pi release. The release of Pi leads to a weakly bound ADP state (state 5). With the increase of external load, forward step of motor becomes difficult to complete before Pi release, while backward step may occur from state 5. If the rear head releases its ADP before it is semidetached from the MT, kinesin-1 in state 5 will return to state 1. Evidently, one ATP is hydrolyzed during cycle 1 → 2→ 5→ 1 but without output of mechanical work, which we called *futile* cycle. As concluded in the study by Clancy et al (40), the inclusion of *futile* cycle is experimentally meaningful and theoretically essential to make the model fit the experimental data well.

Semidetach state 6 is the weakest binding state, and any backward slipping necessarily requires passage through this state. From state 6, kinesin-1 may dissociate completely from the MT and enter into the detachment state, denoted by 'Off' in Figure 1. As stated in the study by Toleikis et al (30), kinesin-1 in state 6 may also slip backward along the MT. Our model assumes that unless it is completely detached from the MT, kinesin-1 always slips backward $d = 8$ nm in each slipping process, then releases the ADP and returns to state 1. This assumption can be relaxed to allow kinesin-1 to slip backward any distance of integer multiple of 8 nm. But results of fitting to experimental data show that the load free rate k_{61}^0 is very small, so the possibility of backward sliding is small, and this simplification is reasonable (see Table 1). Meanwhile, kinesin-1 in semidetach state 6 may also slide forward along the MT. But since the probability of kinesin-1 in state 6 is very small (see Fig. 3), compared with the total forward probability flux, the flux produced by forwarding sliding is negligible.

The model used in this study is similar to the one as presented in the study by Toleikis et al (30). One of the key features distinguishing it from earlier ones is the inclusion of semidetach state 6, from which kinesin-1 can either slip backward to state 1 or dissociate from the MT completely. Generally, biochemical cycles of kinesin-1 in this model can be classified into three categories: **(i)** *forward* cycle coupled with one forward mechanical step, **(ii)** *backward* cycle coupled with one backward mechanical step, and **(iii)** *futile* cycle with one ATP hydrolyzed but without change of position.

As illustrated in Figure 1*A*, biochemical transitions 2 ⇌ 3, 3⇌ 1, and 4⇌ 2 are coupled with head attachment/detachment to/from the MT-binding site, which may result in the change of mass center of kinesin-1. So rates of these transitions, *i.e.*, k_{23}, k_{32}, k_{31}, k_{13}, k_{42}, k_{24}, are assumed to be external load F dependent. Similar as in the studies by Fisher and Kolomeisky (35) and Zhang (41), this study assumes that

$$\begin{aligned} k_{23}(F) &= k_{23}^0 e^{\frac{-\delta_{23}Fd}{k_BT}}, \quad k_{32}(F) = k_{32}^0 e^{\frac{\delta_{32}Fd}{k_BT}}, \\ k_{31}(F) &= k_{31}^0 e^{\frac{-\delta_{31}Fd}{k_BT}}, \quad k_{13}(F) = k_{13}^0 e^{\frac{\delta_{13}Fd}{k_BT}}, \\ k_{42}(F) &= k_{42}^0 e^{\frac{-\delta_{42}Fd}{k_BT}}, \quad k_{24}(F) = k_{24}^0 e^{\frac{\delta_{24}Fd}{k_BT}}, \end{aligned} \tag{1}$$

where k_{ij}^0 are load-free transition rates, F is the external load (positive if it points to the minus end of the MT), k_B is the Boltzmann constant, T is the absolute temperature, and $d = 8$ nm is the step size of kinesin-1. $\delta_{ij} \geq 0$ is called the *load distribution factor* that reflects how external load affects the rate of transition from state i to state j, which satisfies

$$\delta_{23} + \delta_{32} + \delta_{31} + \delta_{13} = 1, \quad \delta_{23} + \delta_{32} + \delta_{42} + \delta_{24} = 1.$$

Since transitions 4 → 2 and 3→ 1 describe the same biochemical process, during which phosphate Pi is released and then the trailing head is detached from the MT, we let $k_{42}^0 = k_{31}^0$ and $k_{24}^0 = k_{13}^0$. However, the position of energy barrier between states 4 and 2 might be different from that between states 3 and 1, so load distribution factors δ_{42}, δ_{24} are generally different from δ_{31}, δ_{13} (1, 35).

The detachment rate k_{off} of kinesin-1 from the MT is assumed to be load F dependent and formulated as $k_{\text{off}}(F) = k_{\text{off}}^0 \exp(Fd_{\text{off}}/k_BT)$, with $d_{\text{off}} \geq 0$ a *characteristic distance*. This expression is actually equivalent to the one used previously in the studies by Müller et al (42) and Zhang and Fisher

(43), where the detachment rate is assumed the be the form $\varepsilon_0 \exp(|F|/F_d)$ with parameter F_d called detachment force. Meanwhile, it is biophysically reasonable to assume the sliding process from states 6 to 1 is load-dependent, and the rate k_{61} is given as $k_{61}(F) = k_{61}^0 \exp(Fd/k_BT)$.

Both transitions 1 → 2 and 3→ 4 describe ATP binding to the nucleotide-free head of kinesin-1. So, rates k_{12} and k_{34} depend on ATP concentration. In our model, we assume $k_{12}(\mathrm{ATP}) = k_{12}^0[\mathrm{ATP}] = k_{34}^0[\mathrm{ATP}] = k_{34}(\mathrm{ATP})$. The inverse transitions 2 → 1 and 4→ 3 describe the disassociation of ATP. So, rates k_{21} and k_{43} are independent of load F and [ATP]. Moreover, we let $k_{21} = k_{43}$.

Rates $k_{25}, k_{52}, k_{51}, k_{15}$ describe the release/recruiting of phosphate Pi or ADP. For simplicity, we assume the change of concentrations of ADP and Pi in environment is negligible, and all these rates are assumed to be constants, though more sophisticated methods can be used to handle their dependence on [ATP] (35).

Data availability

The data for kinesin-1 purified from wildtype *Drosophila* that support the findings of this study are available within the published articles (33, 44), where the data of mean velocity and mean run length are from the study by Schnitzer et al (44), and the data of randomness and stall force are from the study by Visscher et al (33).

Supporting information—This article contains supporting information.

Author contributions—B. S. and Y. Z. conceptualization; B. S. and Y. Z. methodology; B. S. writing–original draft; Y. Z. writing–review and editing.

Conflict of interest—The authors declare that they have no conflicts of interest with the contents of this article.

Abbreviations—The abbreviations used are: MT, microtubule; NL, neck linker.

References

1. Howard, J. (2001) *Mechanics of Motor Proteins and the Cytoskeleton*, Sinauer Associates, Sunderland, MA
2. Vale, R. D. (2003) The molecular motor toolbox for intracellular transport. *Cell* **112**, 467
3. Schliwa, M. (2003) *Molecular Motors*, Wiley-Vch, Weinheim
4. Kolomeisky, A. B. (2015) *Motor Proteins and Molecular Motors*, CRC Press, Taylor & Francis Group, Boca Raton, FL
5. Case, R. B., Rice, S., Hart, C. L., Ly, B., and Vale, R. D. (2000) Role of the kinesin neck linker and catalytic core in microtubulebased motility. *Curr. Biol.* **380**, 157
6. Al-Bassam, J., Cui, Y., Klopfenstein, D., Carragher, B. O., Vale, R. D., and Milligan, R. A. (2003) Distinct conformations of the kinesin Unc104 neck regulate a monomer to dimer motor transition. *J. Cell Biol.* **163**, 743
7. Tomishige, M., Stuurman, N., and Vale, R. D. (2006) Single-molecule observations of neck linker conformational changes in the kinesin motor protein. *Nat. Struct. Mol. Biol.* **13**, 887
8. Kalchishkova, N., and Böhm, K. J. (2008) The role of kinesin neck linker and neck in velocity regulation. *J. Mol. Biol.* **382**, 127
9. Hariharan, V., and Hancock, W. O. (2009) Insights into the mechanical properties of the kinesin neck linker domain from sequence analysis and molecular dynamics simulations. *Cell Mol. Bioeng.* **2**, 177
10. Asbury, C. L., Fehr, A. N., and Block, S. M. (2003) Kinesin moves by an asymmetric hand-over-hand mechanism. *Science* **302**, 2130
11. Yildiz, A., Tomishige, M., Vale, R. D., and Selvin, P. R. (2004) Kinesin walks hand-over-hand. *Science* **303**, 676
12. Schnitzer, M. J., and Block, S. M. (1997) Kinesin hydrolyses one ATP per 8-nm step. *Nature* **388**, 386
13. Coy, D. L., Wagenbach, M., and Howard, J. (1999) Kinesin takes one 8-nm step for each ATP that it hydrolyzes. *J. Biol. Chem.* **274**, 3667
14. Svoboda, K., Schmidt, C. F., Schnapp, B. J., and Block, S. M. (1993) Direct observation of kinesin stepping by optical trapping interferometry. *Nature* **365**, 721
15. Higuchi, H., Bronner, C. E., Park, H. W., and Endow, S. A. (2004) Rapid double 8-nm steps by a kinesin mutant. *EMBO J.* **23**, 2993
16. Guydosh, N. R., and Block, S. M. (2009) Direct observation of the binding state of the kinesin head to the microtubule. *Nature* **461**, 125
17. Carter, N. J., and Cross, R. A. (2005) Mechanics of the kinesin step. *Nature* **435**, 308
18. Toprak, E., Yildiz, A., Hoffman, M. T., Rosenfeld, S. S., and Selvin, P. R. (2009) Why kinesin is so processive. *Proc. Natl. Acad. Sci. U. S. A.* **106**, 12717
19. Clancy, B. E., Behnke-Parks, W. M., Andreasson, J. O., Rosenfeld, S. S., and Block, S. M. (2011a) A universal pathway for kinesin stepping. *Nat. Struct. Mol. Biol.* **18**, 1020
20. Ariga, T., Tomishige, M., and Mizuno, D. (2018) Nonequilibrium energetics of molecular motor kinesin. *Phys. Rev. Lett.* **121**, 218101
21. Svoboda, K., and Block, S. M. (1994) Force and velocity measured for single kinesin molecules. *Cell* **77**, 773
22. Visscher, K., Schnitzer, M. J., and Block, S. M. (1999a) Single kinesin molecules studied with a molecular force clamp. *Nature* **400**, 184
23. Block, S. M., Asbury, C. L., Shaevitz, J. W., and Lang, M. J. (2003) Probing the kinesin reaction cycle with a 2D optical force clamp. *Proc. Natl. Acad. Sci. U. S. A.* **100**, 2351
24. Parrondo, J. M. R., and Cisneros, B. J. D. (2002) Energetics of brownian motors: a review. *Appl. Phys. A.* **75**, 179
25. Kolomeisky, A. B., and Fisher, M. E. (2007) Molecular motors: A theorist's perspective. *Ann. Rev. Phys. Chem.* **58**, 675
26. Chowdhury, D. (2013) Stochastic mechano-chemical kinetics of molecular motors: A multidisciplinary enterprise from a physicist perspective. *Phys. Rep.* **529**, 1
27. Mugnai, M. L., Hyeon, C., Hinczewski, M., and Thirumalai, D. (2020) Theoretical perspectives on biological machines. *Rev. Mod. Phys.* **92**, 025001
28. Kampen, N. G. V. (2007) *Stochastic Processes in Physics and Chemistry*, Elsevier Science & Technology Books, North-Holland, Netherlands
29. Gardiner, C. W. (2010) *Handbook of Stochastic Methods*, Springer-Verlag, Berlin Heidelberg, Germany
30. Toleikis, A., Carter, N. J., and Cross, R. A. (2020) Backstepping mechanism of kinesin-1. *Biophys. J.* **119**, 1984
31. Coppin, C. M., Finer, J. T., Spudich, J. A., and Vale, R. D. (1996) Detection of sub-8-nm movements of kinesin by high-resolution optical-trap microscopy. *Proc. Natl. Acad. Sci. U. S. A.* **93**, 1913
32. Nishiyama, M., Muto, E., Inoue, Y., Yanagida, T., and Higuchi, H. (2001) Substeps within the 8-nm step of the ATPase cycle of single kinesin molecules. *Nat. Cell Biol.* **3**, 425
33. Visscher, K., Schnitzer, M. J., and Block, S. M. (1999b) Single kinesin molecules studied with a molecular force clam. *Nature* **400**, 184
34. Coppin, C. M., Pierce, D. W., Hsu, L., and Vale, R. D. (1997) The load dependence of kinesin's mechanical cycle. *Proc. Natl. Acad. Sci. U. S. A.* **94**, 8539
35. Fisher, M. E., and Kolomeisky, A. B. (2001) Simple mechanochemistry describes the dynamics of kinesin molecules. *Proc. Natl. Acad. Sci. U. S. A.* **98**, 7748
36. Toba, S., Watanabe, T. M., Yamaguchi-Okimoto, L., Toyoshima, Y. Y., and Higuchi, H. (2006) Overlapping hand-over-hand mechanism of single molecular motility of cytoplasmic dynein. *Proc. Natl. Acad. Sci. U. S. A.* **103**, 5741

37. Astumian, R. D. (1997) Thermodynamics and kinetics of a Brownian motor. *Science* **276**, 917
38. Zhang, Y. (2008) Three phase model of the processive motor protein kinesin. *Biophys. Chem.* **136**, 19
39. Block, S. M. (2007) Kinesin motor mechanics: binding, stepping, tracking, gating, and limping. *Biophys. J.* **92**, 2986
40. Clancy, B. E., Behnke-Parks, W. M., Andreasson, J. O., Rosenfeld, S. S., and Block, S. M. (2011) A universal pathway for kinesin stepping. *Nat. Struct. Mol. Biol.* **18**, 1020
41. Zhang, Y. (2012) Phenomenological analysis of ATP dependence of motor proteins. *PLoS One* **7**, e32717
42. Müller, M. J. I., Klumpp, S., and Lipowsky, R. (2008) Tug-of-war as a cooperative mechanism for bidirectional cargo transport by molecular motors. *Proc. Natl. Acad. Sci. U. S. A.* **105**, 4609
43. Zhang, Y., and Fisher, M. E. (2010) Dynamics of the tugof- war model for cellular transport. *Phys. Rev. E* **82**, 011923
44. Schnitzer, M. J., Visscher, K., and Block, S. M. (2000) Force production by single kinesin motors. *Nat. Cell Biol.* **2**, 718